$$A_1 = 1.6\ \text{kgf/m}^2 \text{ and } 0.05 < A_2 < 0.3\ \text{kgf/m}^2$$

Since the rubber rod cannot expand in the y direction, $\lambda_y = 1$. Furthermore, if we assume that the rubber is incompressible, then[2] $\lambda_x\lambda_y\lambda_z = 1$. Inserting $\lambda_y = 1$ into this expression gives $\lambda_z = 1/\lambda_x$. Inserting the last expression into Eq. (15) and replacing λ_x and σ_x by λ and σ_2 respectively results in

$$\sigma_2 = (A_1 + A_2)\left(\lambda - \frac{1}{\lambda^3}\right) \tag{16}$$

which satisfies Eq. (2) if one defines $G_2 = (A_1 + A_2)$. The remaining development for two-dimensional compression is identical to the one given earlier with $n = 2$ rather than $n = 1$, which gives the appropriate expressions for a one-dimensional compression.

Discussion and Conclusions

The location along a rubber rod where the compression wave generated upon an impact on one of its edges has been calculated for one- and two-dimensional compression. The case of a three-dimensional compression could not be solved due to lack of an expression relating the stress to the strain.

Comparing Eq. (12) for $n = 1$ and $n = 2$ by calculating the velocity of the first Riemann wave (the values of the various physical constants are taken from Ref. 5) indicates that for a one-dimensional compression,

$$(C_0)_1 = 46.37\ \text{m/s}$$

while for a two-dimensional compression

$$26.37 < (C_0)_2 < 28.29\ \text{m/s}$$

where the lower and upper limits correspond to the smaller and higher values of A_2 respectively. Thus, as can be seen, the first Riemann wave, i.e., the velocity and the head of the compression wave in a two-dimensional compression, travels at about 60% the velocity of the head of the compression wave in the case of a one-dimensional compression. This suggests that for the same impact conditions, a shock wave will be formed much earlier when the rubber rod can expand only in one direction.

From Eq. (14) one can get

$$\frac{(x_s)_2}{(x_s)_1} = \left[\frac{(C_0)_2}{(C_0)_1}\right]^2$$

and since $(C_0)_2 \approx 0.6(C_0)_1$ one obtains $(x_s)_2 \approx 0.36(x_s)_1$, which means that the distance where a shock wave is formed in a rubber rod under a two-dimensional compression is about one-third the distance needed for a shock wave to be formed when the rubber rod is only under a one-dimensional compression.

References

[1]Courant, R. and Friedricks, K. O., *Supersonic Flow and Shock Waves*, Vol. 1, Interscience Publications Inc., New York, London, 1948.

[2]Treloar, L. R. G., *The Physics of Rubber Elasticity*, Oxford at the Clarendon Press, Oxford, 1949.

[3]Nowinski, J. L., "On the Propagation of Finite Disturbances in Bars of Rubberlike Materials," *Journal of Engineering for Industry*, Vol. 87, 1965, pp. 523–529.

[4]Glass, I. I. and Hall, J. G., "Shock Tubes," *Handbook of Supersonic Aerodynamics*, Vol. 6, Sec. 48, NAVORD Rept. 1488, 1959.

[5]Kolsky, H., *Stress Waves in Solids*, Dover Publications Inc., New York, 1952.

Hybrid Finite-Element Analysis of Laplace's Equation with Singularities

Kuen Ting* and Wen-Hwa Chen†

National Tsing Hua University, Hsinchu, Taiwan

Introduction

THIS Note is devoted to solving Laplace's equation subjected to appropriate boundary conditions with singularities. Earlier attempts to solve this problem using finite-element techniques used conventional elements[1] or quarter-point singular elements.[2,3] Although those elements were easily used in available finite-element packages, a rather refined mesh needed to be employed. Several investigators[4,5] then created a special singular element to model the region near the singular point, but did not satisfy the condition of continuity for the independent variables in partial differential equations. Recently, the global element method[6,7] for which shape functions with an embedded singularity have been devised for this problem with relatively simple domains (e.g., circles, squares, etc.). Thus, it would be preferable to construct a finite-element model that can be used to solve the Laplace equation with complicated geometries such that singularities are considered in several special elemens surrounding the singular point and conditions of continuity of solutions at the interelement boundaries are still satisfied. The hybrid finite-element models developed by the authors[8,9] in dealing with thermoelastic fracture problems seem to be good choices for this purpose.

Motz's Problem

As shown in Fig. 1, without loss of generality, the problem first introduced by Motz[10] is chosen as the example to tackle: The problem is governed by the two-dimensional Laplace equation

$$\nabla^2 u = 0 \text{ in R}$$

subjected to the boundary conditions

$$u = f_1 \text{ on OP}$$

$$= f_2 \text{ on BC}$$

and

$$\frac{\partial u}{\partial n} = g \text{ on AB, AD, CD}$$

where $\partial u/\partial n$ is the outward normal gradient of u, and f_1, f_2, and g are constants.

Hybrid Finite-Element Analysis

The variational principle that governs the hybrid finite-element models for thermoelastic fracture problems can be further generalized as follows:

$$\pi(u, \tilde{u}, \tilde{\lambda}_n) = \sum_m \left\{ \int_{A_m} \frac{1}{2}(\nabla u)^T(\nabla u)\mathrm{d}A + \int_{S_{hm}} g\tilde{u}\mathrm{d}s \right.$$

Received Nov. 13, 1986; revision received Feb. 18, 1987.

*Graduate Student, Department of Power Mechanical Engineering.

†Professor and Head, Department of Power Mechanical Engineering.

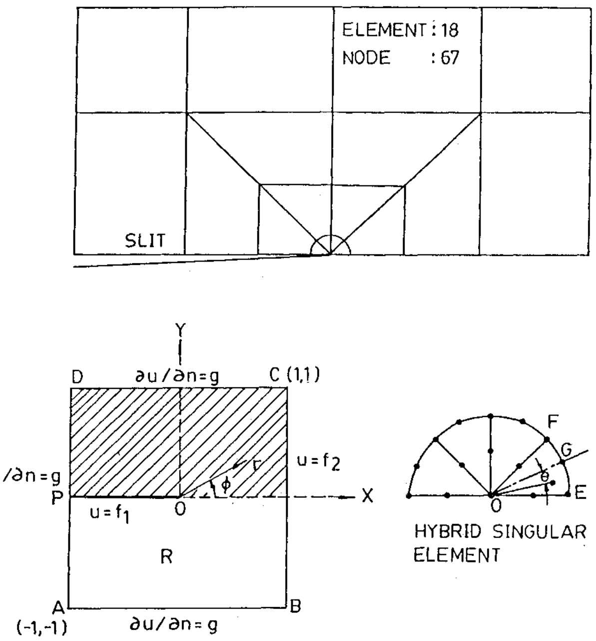

Fig. 1 Finite-element mesh for Motz's problem.

$$- \int_{\partial A_m} \tilde{\lambda}_n (\tilde{u}-u) \mathrm{d}s \Big\} = \min \tag{1}$$

Here A_m is the area of element m in the finite region R; ∂A_m the boundary of A_m; S_{hm} the portion of ∂A_m in which the outward normal gradient of u is prescribed, say, $\partial u/\partial n = g$; the element interior variable u is differentiable within A_m but need not satisfy a priori interelement continuity. The variable $\tilde{u}$ is the interelement boundary variable that satisfies the boundary condition $\tilde{u}=f$ on S_{um}. S_{um} is the portion of ∂A_m in which the value of u is prescribed. $\tilde{\lambda}_n$ is the Lagrangian multiplier, which is physically the interelement boundary outward normal gradient of u on ∂A_m. After checking the Euler equations and natural boundary conditions corresponding to $\delta\pi = 0$, the interelement continuity of variable u between two adjacent elements is still enforced. Thus, the correct singularities[8,9] can be freely embedded in several hybrid singular elements around the point O and, for simplicity, conventional isoparametric elements are taken elsewhere.

For the present finite-element implementations, u, $\tilde{u}$, and $\tilde{\lambda}_n$ in Eq. (1) can be assumed in terms of column vectors of parameters α, β, and the nodal value q, respectively,

$$u = \{U\}^T \{\beta\} \text{ in } A_m \tag{2}$$

$$\tilde{u} = \{L\}^T \{q\} \text{ on } \partial A_m \tag{3}$$

$$\tilde{\lambda}_n = \{\mathrm{R}\}^T \{\alpha\} \text{ on } \partial A_m \tag{4}$$

where $\{\ \}^T$ denotes the transpose of the column vector $\{\ \}$. The interpolation functions $\{U\}^T$, $\{L\}^T$, and $\{R\}^T$ will be discussed in the appendix. Substituting Eqs. (2-4) into Eq. (1) and performing the necessary manipulations, the final algebraic system equations are derived as

$$[K^*]\{q^*\} = \{Q^*\}$$

where $[K^*]$, $\{q^*\}$, and $\{Q^*\}$ represent the corresponding global matrix of stiffness, nodal value, and loading vectors, respectively.

Results

For comparison purposes, the constants f_1, f_2, and g given in Motz's problem are taken as 0, 500, and 0, respectively. Due to symmetry, it is sufficient to solve the shaded area whose finite-element mesh is displayed in Fig. 1. Four circular sector-shaped hybrid singular elements are surrounded by 14 eight-node isoparametric elements, and 67 degrees of freedom are used. The results obtained at the grid points are given in Table 1, where they are compared with the results of Refs. 3, 5, 6, 11, and 12. Good correlations between the present results and the referenced solutions are found. It is worthwhile to note that a total of 451 degrees of freedom were taken in Wait's model[3] (using quarter-point singular elements) vs the 67 degrees of freedom used in the present hybrid finite-element method. Figure 2 shows the contours of solution u of Motz's problem. Excellent results at the boundaries are also observed.

Appendix

Assumed Element Interior Variable u

Based on the results of the authors' previous works,[8,9] the interpolation function of the element interior variable u in Eq. (2) can be derived as

$$\{U\}^T = [1,\ r\phi,\ r^{1/2}\sin(\phi/2),\ r\sin\phi,\ r^{3/2}\sin(3/2)\phi,$$

$$r^2\sin 2\phi,\ r^{5/2}\sin(5/2)\phi,\ r^3\sin 3\phi,\ r^{7/2}\sin(7/2)\phi,$$

Table 1 Solution of Motz's problem

(x,y)	Present	Hendry and Delves[6]	Whiteman[11]	Morely[5]	Wait[3]	Wait and Mitchell[12]
(−1/7,1/7)	61.9	—	62.0	—	61.8	61.4
(−1/14,1/7)	78.8	—	78.8	—	78.8	78.3
(0,1/7)	103.9	—	103.8	—	103.5	103.3
(1/14,1/7)	135.8	—	135.7	—	135.5	134.3
(1/7,1/7)	169.4	—	169.5	—	169.2	168.2
(0,3/28)	90.5	—	90.6	—	90.4	89.7
(−3/28,1/14)	33.5	—	33.4	—	33.2	32.8
(0,1/14)	74.9	—	74.6	—	74.4	73.3
(1/7,1/14)	160.4	—	160.4	—	160.3	159.0
(0,1/28)	53.2	53.2	53.2	53.1	53.2	51.4
(1/28,0)	76.6	—	76.4	—	76.4	76.4
(1/14,0)	109.3	—	108.9	—	108.6	106.9
(3/28,0)	134.2	—	134.4	—	134.2	132.9
(1/7,0)	156.7	—	156.5	—	156.2	156.6
(0,4/7)	183.9	183.9	—	—	—	183.5
(4/7,4/7)	356.7	356.7	—	—	—	356.9

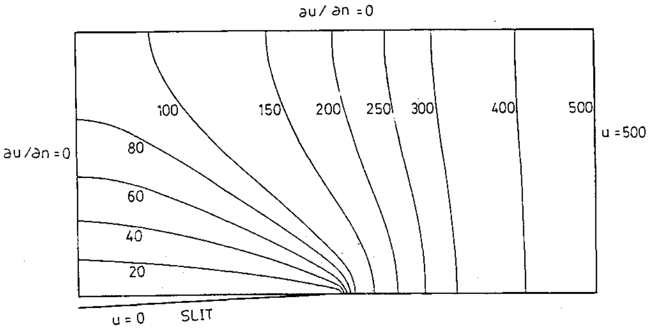

Fig. 2 Constant contours of solutions of Motz's problem.

$$r^{1/2}\cos(\phi/2),\ r\cos\phi,\ r^{3/2}\cos(3/2)\phi,\ r^2\cos 2\phi,$$

$$r^{5/2}\cos(5/2)\phi,\ r^3\cos 3\phi,\ r^{7/2}\cos(7/2)\phi]_{1\times 16}$$

and

$$\{\beta\}^T=[\beta_1,\beta_2,\ldots,\beta_{16}]$$

where (r,ϕ) are the polar coordinates centered at the singular point O.

Assumed Element Boundary Variable $\tilde{u}$

The element boundary variable u should have the same value at the common boundaries of adjacent elements. Hence, $\tilde{u}$ in Eq. (3) is assumed to be (see Fig. 1):

Along EF:

$$u=a_1+a_2\theta+a_3\theta^2$$

Along OE or OF:

$$u=a_4+a_5r^{1/2}+a_6r$$

where θ is the local coordinate with respect to the central axis OG. The parameters $(a_1,a_2,\ldots,a_6)$ can be uniquely determined in terms of nodal values of $\{q\}$, and $\{L\}^T$ is then obtained.

Lagrangian Multiplier $\tilde{\lambda}_n$

To ensure a better approximation, the independently assumed Lagrangian multiplier $\tilde{\lambda}_n$ along the boundaries can be generated from the gradient of u, λ_i, which satisfies the following equations:

$$\lambda_{i,i}=0 \text{ on } \partial A_m \qquad \text{(A1)}$$

$$\tilde{\lambda}_n=\lambda_i n_i \text{ on } \partial A_m \qquad \text{(A2)}$$

Since the assumed variable u contains $r^{1/2}$-type behavior[8,9] $\tilde{\lambda}_n$ will generate a $r^{-1/2}$ singular behavior along the boundary ∂A_m. The radial and tangential components of λ_i, λ_r, and λ_ϕ can be taken as

$$\begin{aligned}\lambda_r=&\alpha_1+\alpha_2 r+\alpha_3 r^{-1/2}\sin(\phi/2)+\alpha_4\sin\phi\\&+\alpha_5 r^{1/2}\sin(3/2)\phi+\alpha_6 r\sin 2\phi+\alpha_7 r^3\sin(5/2)\phi\\&+\alpha_8 r^2\sin 3\phi+\alpha_9 r^{5/2}\sin(7/2)\phi+\alpha_{10}r^{-1/2}\cos(\phi/2)\\&+\alpha_{11}\cos\phi+\alpha_{12}r^{1/2}\cos(3/2)\phi+\alpha_{13}r\cos 2\phi\\&+\alpha_{14}r^{3/2}\cos(5/2)\phi+\alpha_{15}r^2\cos 3\phi+\alpha_{16}r^{5/2}\cos(7/2)\phi\end{aligned}$$

and

$$\begin{aligned}\alpha_\phi=&-\alpha_1\phi-2\alpha_2 r\phi+\alpha_3 r^{-1/2}\cos(\phi/2)+\alpha_4\cos\phi\\&+\alpha_5 r^{1/2}\cos(3/2)\phi+\alpha_6 r\cos 2\phi+\alpha_7 r^{3/2}\cos(5/2)\phi\\&+\alpha_8 r^2\cos 3\phi+\alpha_9 r^{5/2}\cos(7/2)\phi-\alpha_{10}r^{-1/2}\sin(\phi/2)\\&-\alpha_{11}\sin\phi-\alpha_{12}r^{1/2}\sin(3/2)\phi-\alpha_{13}r\sin 2\phi\\&-\alpha_{14}r^{3/2}\sin(5/2)\phi-\alpha_{15}r^2\sin 3\phi-\alpha_{16}r^{5/2}\sin(7/2)\phi\end{aligned}$$

As a result, from Eqs. (A1) and (A2), the assumed interpolation function $\{R\}^T$ of $\tilde{\lambda}_n$ can be easily determined.

References

[1]Thatcher, R. W., "Singularities in the Solution of Laplace's Equation in Two Dimensions," *Journal of Institutive Mathematics and Applications*, Vol. 16, 1975, pp. 303–319.

[2]Wait, R., "Singular Isoparametric Finite Elements," *Journal of Institutive Mathematics and Applications*, Vol. 20, 1977, pp. 133–141.

[3]Wait, R., "A Curved Macro-Element for Cracks and Corners," *Journal of Institutive Mathematics and Applications*, Vol. 24, 1979, pp. 471–480.

[4]Wait, R., "Finite Element Methods for Elliptic Problems with Singularities," *Computer Methods in Applied Mechanics and Engineering*, Vol. 13, 1978, pp. 141–150.

[5]Morley, L. S. D., "Finite Element Solution of Boundary-Value Problems with Non-removable Singularities," *Philosophical Transactions of the Royal Society of London*, Vol. A275, 1973, pp. 463–488.

[6]Hendry, J. A. and Delves, L. M., "The Global Element Method Applied to a Harmonic Mixed Boundary Value Problem," *Journal of Computational Physics*, Vol. 33, 1979, pp. 33–44.

[7]Kermode, M., McKerrell, A., and Delves, L. M., "Calculation of Singular Coefficients," *Computer Methods in Applied Mechanics and Engineering*, Vol. 50, 1985, pp. 205–215.

[8]Chen, W. H. and Ting, K., "Finite Element Analysis of Mixed-Mode Thermoelastic Fracture Problems," *Nuclear Engineering and Design*, Vol. 90, 1985, pp. 55–65.

[9]Chen, W. H. and Ting, K., "Finite Element Analysis of Transient Thermoelastic Fracture Problems," *Proceedings of International Conference on Computational Mechanics*, Tokyo, Japan, May 1986, Vol. 2, pp. V79–85.

[10]Motz, H., "The Treatment of Singularities of Partial Differential Equations by Relaxation Methods, *Quarterly Journal of Applied Mathematics*, Vol. 4, 1946, pp. 371–377.

[11]Whiteman, J. R., "Numerical Solution of a Harmonic Mixed Boundary Value Problem by the Extension of a Dual Series Method," *Quarterly Journal of Mechanics and Applied Mathematics*, Vol. 23, 1970, pp. 449–455.

[12]Wait, R. and Mitchell, A. R., "Corner Singularities in Elliptic Problems by Finite Element Methods," *Journal of Computational Physics*, Vol. 8, 1971, pp. 45–52.